

Closed universe and the first Doppler-peak of the CMB spectrum

Sergio del Campo¹

¹ *Instituto de Física, Universidad Católica de Valparaíso,
Av Brasil 2950, Valparaíso, Chile.*

31 October 2018

ABSTRACT

We study universe models which are intrinsically closed and are full of a quintessence scalar field, besides the Cold Dark Matter component. We use these to depict diverse flat Cold Dark Matter models. With the background geometry specified by the Friedman-Robertson-Walker metric, we include among them the standard Cold Dark Matter, the Cosmological Constant Cold Dark Matter and the Dark Energy or Quintessence Cold Dark Matter models. After describing these models, we determine the position of the first Doppler peak of the Cosmic Microwave Background anisotropy spectrum for Ω_T close to one; we also study the shift parameter R .

Key words: cosmology: theory – early Universe – cosmological parameters – cosmic microwave background.

1 INTRODUCTION

To day, we do not know precisely the exact amount of matter present in the universe, so that we ignore its geometry. Astronomical observations conclude that the matter density related to baryonic and nonbaryonic cold dark matter is much less than the critical density value (White et al. 1993). However, recent measurements of type Ia distant supernova indicate that in the universe there exists an important energy component which contributes to a large component of negative pressure, and thus it accelerates rather than decelerates the universe (Perlmutter et al.1998; Garnavich et al. 1998).

Different interpretations have been suggested for explaining the acceleration of the universe. We distinguish here those related to the existence of a cosmological constant, and the quintessence or dark energy models. The former are characterized by a vacuum energy density, while the latter are characterized by a scalar field χ , and its potential $V(\chi)$ (Caldwell, Dave & Steinhardt 1998).

Various tests of cosmological models, including space-time geometry, galaxy peculiar velocities, structure formation, and very early universe descriptions (related to inflation (Guth1981)) support a flat universe scenario. Specifically, the redshift-distant relation for supernova of type Ia, anisotropies in the cosmic microwave background radiation (Roos & Harun 2000; Mather et al. 1994) and gravitational lensing (Mellier 1999) suggest that $\Omega_T = 1.00 \pm 0.12$ (95% *cl*) (De Bernardis et al. 2000).

In light of these results, one interesting question to ask is whether this flatness is due to a sort of compensation

among different components that enter into the dynamical equations. In the literature we find some descriptions along these lines. For instance, a closed model with an important matter component with equation of state given by $P = -\rho/3$ has been studied (Kolb 1989). Here, the universe expands at a constant speed. Other authors, using the same equation of state, have added a nonrelativistic component in which the total matter density, Ω_T , is less than one, thus describing an open universe (Kamionkowsky & Toumbas 1996). Also, flat decelerating universe models have been simulated (Cruz, del Campo & Herrera 1998; Cataldo & del Campo 2000; del Campo & Cruz 2000). The common fact in all of these models is that, even though the starting geometry were other than that corresponding to the critical geometry, all of these models are indistinguishable from flat models at low redshift.

In this work we want to describe a closed universe model composed of two matter components. One is the usual non-relativistic dust matter and the other corresponds to a sort of quintessence-type matter, designated by the Q scalar field, which we assume obeys an equation of state

$$P_Q = w_Q \rho_Q, \quad (1)$$

where, in general, the w_Q parameter is a time dependent negative. We also assume that its current value is bounded from the above, $w_Q \leq -1/3$. The geometry, together with this matter component, combines in a way such that flat universe scenarios arise. Among the scenarios which we consider are the standard Cold Dark Matter or Einstein-de Sitter (sCDM), the Cosmological Constant Cold Dark Matter (Λ CDM) and the Quintessence (or dark energy) Cold Dark

arXiv:astro-ph/0211407v1 18 Nov 2002

Matter (χ CDM) models. In the latter scenario, a scalar field χ is added to the relevant components (Wang, Caldwell, Ostriker & Steinhardt 2000). In this case, it is assumed that there exists an equation of state for the dark energy scalar field χ given by $P_\chi = w_\chi \rho_\chi$, where astronomical observations (related to type Ia supernovae measurements) set an upper limit on the present value of w_χ , $w_\chi \leq -1/3$ (Garavich et al. 1998).

From the theoretical point of view, anisotropies in the CMB are related to small perturbations, which are believed to seed the formation of large-scale structures in the universe. These anisotropies are sensitive to cosmological parameters such as the CDM, number of baryons, three-space curvature and the cosmological constant (Hu & Sugiyama 1995a). These anisotropies are enhanced by oscillations of the photon-baryon fluid before decoupling, which are driven by primordial density fluctuations that depend on the matter content (Hu, Sugiyama & Silk 1997).

Models with adiabatic and isocurvature fluctuations predict a sequence of peaks in the power spectrum which are generated by acoustic oscillations of the photon-baryon fluid at recombination. The fluctuations, as a function of the wavenumber k go as $\cos(kc_s\tau_{LS})$ at last scattering, where c_s is the sound speed and τ_{LS} is the conformal time at recombination. In the case of primordial adiabatic fluctuations, these causes a harmonic series of temperature fluctuation peaks, where $k_m = \frac{m\pi}{c_s\tau_{LS}}$ corresponds to the m th peak. In the isocurvature case, it is found that the acoustic peaks are 90° degrees out of phase with their adiabatic counterparts (Hu & Sugiyama 1995b).

Of particular interest is the height and position of the main acoustic peak - the so called Doppler peak. This pronounced peak in the angular power spectrum occurs at multiple l_{LS} . The exact value of l_{LS} depends on both the linear size of the acoustic horizon and the angular diameter distance from the observer to the recombination era (last scattering surface). Both of these quantities are sensitive to a number of cosmological parameters, essentially to the total density parameter Ω_T , which is defined to be the ratio between the total matter density and the critical energy density. In the case in which there is no contribution from the cosmological constant, it is found that $l_{LS} \sim 200/\sqrt{\Omega_T}$ (Kamionkowsky, Spergel & Sugiyama 1994; Hu & Sugiyama 1995a; Frampton, Ng & Rohm 1998; Dodelsol & Knox 2000; Crooks, Dunn, Frampton & Ng 2000).

A precise measurement of l_{LS} can efficiently constrain the density parameter and, specifically, the curvature of the universe. In fact, in the BOOMERanG (Balloon Observations Of Millimeter Extragalactic Radiation and Geomagnetic) experiment the value $l_{LS} = (197 \pm 6) (1 - \sigma \text{ error})$ has been reported (De Bernardis et al. 2000). This, in a model with $\Lambda = 0$, is consistent with an almost flat geometry, since this value leads to $\Omega_T = 1.03 \pm 0.06$ (Roos & Harun 2000) when the above expression, $l_{LS} \sim \Omega_T^{-1/2}$, is used. For instance, in the case of the Λ CDM model, we find that $\Omega_T = \Omega_M + \Omega_\Lambda$, in which $\Omega_M \equiv \frac{\rho_M^0}{\rho_C} = \left(\frac{8\pi G}{3H_0^2}\right) \rho_M^0$ and $\Omega_\Lambda \equiv \left(\frac{\Lambda}{8\pi G}\right) \frac{1}{\rho_C} = \frac{\Lambda}{3H_0^2}$. Here, ρ_M^0 , ρ_C and H_0 are the present values of the nonrelativistic matter, the critical densities and the Hubble constant, respectively, and G is

the Newton constant. Ω_Λ and Ω_M are parameters associated with the cosmological constant Λ , and the matter density is related to the baryonic and nonbaryonic Cold Dark Matter density, respectively. From now on, all quantities with upper (or lower) zero indexes specify its current values, and we take $c = 1$ for the speed of light.

The paper is presented as follows: In section II we write the Einstein field equations. In section III we study three specific models. They are the sCDM, the Λ CDM, and the χ CDM. In section IV we proceed to describe the position of the first Doppler peak for each of these models. Here, we express the first Doppler peak l_{LS} , in terms of the Ω_T parameter, considered to be close to one. We also determine the shift parameter R for the models studied here. We conclude in section V.

2 THE EINSTEIN FIELD EQUATIONS

We start with the effective Einstein action given by

$$S = \int d^4x \sqrt{-g} \left[\frac{1}{16\pi G} \mathcal{R} + \frac{1}{2} (\partial_\mu Q)^2 - V(Q) + \mathcal{L}_M \right], \quad (2)$$

where \mathcal{R} is the scalar curvature; $V(Q)$ is the scalar potential associated with the scalar field Q ; and \mathcal{L}_M is related to any other matter component.

We shall assume that the Q field is homogeneous, i.e. it is a time-dependent quantity only, $Q = Q(t)$; and the spacetime is isotropic and homogeneous with its metric corresponding to the FRW metric:

$$ds^2 = dt^2 - a(t)^2 \left[\frac{dr^2}{1 - kr^2} + r^2 (d\theta^2 + \sin^2\theta d\phi^2) \right], \quad (3)$$

where $a(t)$ represents the scale factor, and the k parameter takes the values $k = -1, 0, 1$ corresponding to an open, flat and closed three-geometry, respectively. With these assumptions, action (2) yields the following field equations: The time-time component of the Einstein equations reads:

$$H^2 = \frac{8\pi G}{3} (\rho_M + \rho_Q) - \frac{k}{a^2}, \quad (4)$$

and the evolution equation for the Q scalar field becomes

$$\ddot{Q} + 3H\dot{Q} = -\frac{\partial V(Q)}{\partial Q}. \quad (5)$$

Here the overdots denote derivatives with respect to t ; $H = \frac{\dot{a}}{a}$ defines the Hubble expansion rate; ρ_M and ρ_Q are the effective matter energy density and the average energy density related to Q , respectively. The Q -energy density is defined by

$$\rho_Q = \frac{1}{2}\dot{Q}^2 + V(Q). \quad (6)$$

We introduce its average pressure P_Q by means of

$$P_Q = \frac{1}{2}\dot{Q}^2 - V(Q). \quad (7)$$

These two quantities are related by the equation of state, eq. (1). By using eqs. 6 and 7, eq. (5) becomes

$$\dot{\rho}_Q + 3H(\rho_Q + P_Q) = 0, \quad (8)$$

which represents an energy balance for the scalar field Q . Similarly, we have a relation for the nonrelativistic matter component, i.e. $\dot{\rho}_M + 3H(\rho_M + P_M) = 0$, which we take to be characterized by the equation of state $P_M = 0$, corresponding to a nonrelativistic dust component, in which case this equation solves to give: $\rho_M \propto a^{-3}$. In this way, we have a combination of two noninteracting perfect fluids: the dust matter component (ρ_M) and the quintessence scalar field (ρ_Q) component.

Equation (4) may be written as

$$H^2 = H_0^2 \left[\Omega_M \left(\frac{\rho_M}{\rho_M^0} \right) + \Omega_Q \left(\frac{\rho_Q}{\rho_Q^0} \right) + \Omega_k \left(\frac{a_0}{a} \right)^2 \right]. \quad (9)$$

Here, the present curvature density parameter, Ω_k , and the quintessence (or dark energy) density parameter, Ω_Q , are defined by

$$\Omega_k = -k \left(\frac{1}{a_0 H_0} \right)^2, \quad (10)$$

and

$$\Omega_Q = \left(\frac{8\pi G}{3H_0^2} \right) \rho_Q^0, \quad (11)$$

respectively.

In the next section we study the characteristics of the different models that arise when the nonrelativistic matter component, ρ_M together with equations (4), (5) and the equation of state for the scalar field Q , are considered, so that different flat universe models occur. As was mentioned in the introduction, these models are the sCDM, the Λ CDM and the χ CDM.

In order to mimic a flat universe, we assume that ρ_Q , together with the curvature term, combine in a way such that the following scenarios occur:

$$\frac{8\pi G}{3} \rho_Q(t) - \frac{k}{a^2(t)} \equiv \begin{cases} 0 & \text{for the sCDM mode,} \\ \frac{\Lambda}{3} & \text{for the } \Lambda\text{CDM model,} \\ \frac{8\pi G}{3} \rho_\chi(t) & \text{for the } \chi\text{CDM model.} \end{cases} \quad (12)$$

For future reference we write eq. (12) in terms of the Ω parameters:

$$\Omega_Q \left(\frac{\rho_Q}{\rho_Q^0} \right) + \Omega_k \left(\frac{a_0}{a} \right)^2 \equiv \begin{cases} 0 & \text{for the sCDM mode,} \\ \Omega_\Lambda & \text{for the } \Lambda\text{CDM model,} \\ \Omega_\chi \left(\frac{\rho_\chi}{\rho_\chi^0} \right) & \text{for the } \chi\text{CDM model,} \end{cases} \quad (13)$$

where, similar to the definitions for Ω_M and Ω_Q , we define $\Omega_\chi = \left(\frac{8\pi G}{3H_0^2} \right) \rho_\chi^0$ for the present value of the quintessence density parameter.

Some comments are in order. In the first two cases we could obtain an explicit expression (as a function of cosmological time) for the unknown energy density, ρ_Q , if we know the scale factor $a(t)$ as an explicit function of time. On the contrary, in the third case, we need not only to know the explicit expression for the scale factor, but also the explicit time dependence of the dark energy density ρ_χ . Also, since in the first case the quantity located on the left hand side has to vanish and, considering that the energy density, ρ_Q , can not be negative, we are forced to consider closed geometries ($k = 1$), in which case Ω_k become negative. In the second and third cases we will also consider the geometry to be closed. In this case, we could take a complete range for the scale factor $a(t)$, i. e. $0 \leq a(t) < \infty$.

3 THE SPECIFIC MODELS

In this section we shall impose the conditions under which a closed universe ($k = 1$) may look like a flat universe ($k = 0$) at low redshift. The flat models are characterized by expression (12) (or equivalently eq. (13)).

3.1 The Einstein-de Sitter or Standard Cold Dark Matter (sCDM) Model

In order to have a closed universe, but one which still has a nonrelativistic matter density whose value corresponds to that of a flat universe, we impose the first condition described by equation (12), i.e. $\rho_Q(a) = \frac{3}{8\pi G a^2}$ or, equivalently, from equation (13)

$$\Omega_Q \left(\frac{\rho_Q}{\rho_Q^0} \right) = -\Omega_C \left(\frac{a_0}{a} \right)^2, \quad (14)$$

where Ω_C is the density parameter for a closed universe, i.e. $\Omega_C \equiv \Omega_{k=1} < 0$. Note that equation (14) gives at present time $\Omega_Q = |\Omega_C|$.

When equation (14) is substituted into equation (9), the following expression results: $H^2 = 8\pi G \rho_M / 3$, which gives for a dust dominated universe: $a(t) = a_0 (t/t_0)^{2/3}$. Notice that this expression gives $\Omega_M = 1$ when evaluated at present time.

Now we are in a position to obtain the intrinsic characteristics of the scalar field Q . From expressions (6) and (7), together with the equation of state, eq. (1), we obtain $\dot{Q}(t) = \sqrt{(1+w_Q) \rho_Q(t)}$, which gives $Q(t) = Q_0 (t/t_0)^{1/3}$, where Q_0 is defined by $Q_0 = 3 \sqrt{(1+w_Q) (t_0/a_0^2)}$.

The same set of equations gives $V_Q(t) = (1 - w_Q) \rho_Q(t) / 2 = V_0 (t_0/t)^{4/3}$, where $V_0 = \rho_C \Omega_Q / 2$. These solutions combine in a way such that the scalar potential becomes

$$V_Q(Q) = V_0 \left(\frac{Q_0}{Q} \right)^4, \quad (15)$$

which represents a typical potential for a quintessence scalar field.

In order to satisfy the field equation (5), we need to take $w_Q = -1/3$. With this value for w_Q , the scalar field Q has properties similar to the matter described in references Kolb (1989), Cruz, del Campo & Herrera (1998), and del Campo & Cruz (2000).

3.2 The Lambda Cold Dark Matter Model (Λ CDM)

Following a procedure similar to that of the previous subsection, we take the second of the three constraints specified by equation (13), i.e.

$$\Omega_Q \left(\frac{\rho_Q(t)}{\rho_Q^0} \right) + \Omega_C \left(\frac{a_0}{a(t)} \right)^2 = \Omega_\Lambda, \quad (16)$$

where the parameters Ω_Q , Ω_C and Ω_Λ have already been defined. Equation (16) evaluated at the present epoch, gives $\Omega_Q + \Omega_C = \Omega_\Lambda$. Since $\Omega_C < 0$, we must satisfy $\Omega_Q > \Omega_\Lambda$.

Under condition (16), the time-time component of Einstein equations becomes analogous to that for a flat universe, where the usual matter and the cosmological constant form the main matter components of the model. Thus, equation (9) reads for a nonrelativistic perfect fluid:

$$H^2 = H_0^2 \left[\Omega_\Lambda + \Omega_M \left(\frac{a_0}{a} \right)^3 \right].$$

Notice that, when this expression is evaluated at present time, i.e. $t = t_0$, we obtain $\Omega_M + \Omega_\Lambda \equiv \Omega_T = 1$. For numerical computations we shall take $\Omega_M = 0.35$ and $\Omega_\Lambda = 0.65$. The latter choice agrees with the amount of cosmological constant, $\Omega_\Lambda < 0.7$, constrained by QSO lensing surveys (Kochanck 1996).

Using the definition of the Hubble parameter together with equation (8), we obtain

$$P_Q = -\frac{1}{3a^2} \frac{d}{da} (a^3 \rho_Q), \quad (17)$$

for the effective pressure associated with the Q field. By substituting eq. (16) into eq. (17), we obtain

$$w_Q^{\Lambda CDM}(a) = -\frac{1}{3} \left[\frac{(\Omega_Q - \Omega_\Lambda) (a_0/a)^2 + 3\Omega_\Lambda}{(\Omega_Q - \Omega_\Lambda) (a_0/a)^2 + \Omega_\Lambda} \right], \quad (18)$$

for the equation state parameter w_Q . Notice that the case $\Lambda = 0$ gives $w_Q^{\Lambda CDM}(a) = -1/3 = \text{const.}$, corresponding to the Einstein-de Sitter model described in the previous subsection. For $\Lambda \neq 0$, the parameter $w_Q^{\Lambda CDM}(a)$ is always negative, since in the limit $a \rightarrow 0$, we get $w_Q^{\Lambda CDM} \rightarrow -1/3$ and for $a \rightarrow \infty$, we find $w_Q^{\Lambda CDM} \rightarrow -1$. Thus, the parameter $w_Q^{\Lambda CDM}$ lies in the range $-1 < w_Q^{\Lambda CDM} < -1/3$. Figure 1 shows how the equation of state parameter $w_Q^{\Lambda CDM}$ changes with time, for three different values of the scalar field density parameter, Ω_Q ; and the parameter Ω_Λ fixed at 0.6.

Another interesting characteristic of the quintessence scalar field is the form of its scalar potential, $V(Q)$. In order to determine this form, we consider the definitions (6) and (7) together with the equation of state (1), we obtain

$$V_Q^{\Lambda CDM}(a) = V_Q^0 \left[\frac{3\Omega_\Lambda + 2(\Omega_Q - \Omega_\Lambda) \left(\frac{a_0}{a} \right)^2}{\Omega_\Lambda + 2\Omega_Q} \right], \quad (19)$$

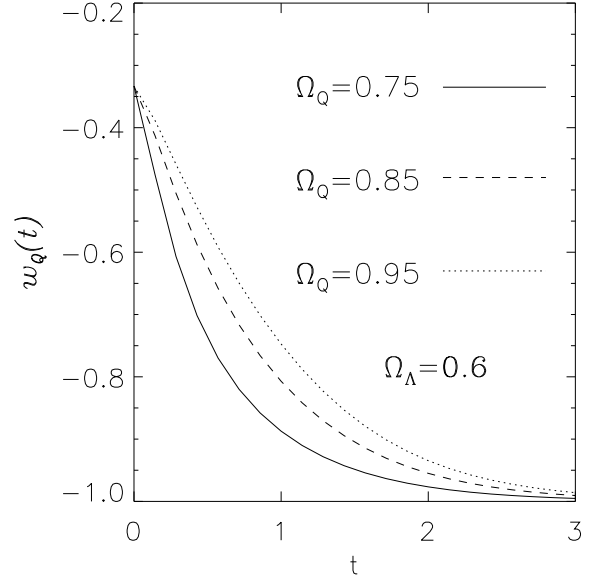


Figure 1. This graph shows the equation of state $w_Q^{\Lambda CDM} = P_Q/\rho_Q$ as a function of time (in units of H_0 , the present value of the Hubble parameter) for three different values of the density parameter, Ω_Q ($\Omega_Q = 0.75, 0.85$ and 0.95). Here, we have used $\Omega_\Lambda = 0.6$.

where $V_Q^0 = \frac{1}{3} \rho_C (\Omega_\Lambda + 2\Omega_Q) \equiv \bar{V}_Q (\Omega_\Lambda + 2\Omega_Q)$ represents the present value of this potential.

On the other hand, from the same equations (6) and (7) we get that, after substituting the corresponding expressions for ρ_Q and w_Q , an explicit expression for the scalar field Q as a function of the scale factor

$$Q(a) = Q_0 \left(\frac{a}{a_0} \right)^{1/2} \times \left[\frac{{}_2F_1 \left(\frac{1}{2}, \frac{1}{6}, \frac{7}{6}; -\left(\frac{\Omega_\Lambda}{\Omega_M} \right) \left(\frac{a}{a_0} \right)^3 \right)}{{}_2F_1 \left(\frac{1}{2}, \frac{1}{6}, \frac{7}{6}; -\left(\frac{\Omega_\Lambda}{\Omega_M} \right) \right)} \right], \quad (20)$$

where ${}_2F_1$ is the generalized hypergeometric function and Q_0 is defined as $Q_0 = Q(a_0) = \bar{Q} \sqrt{\frac{\Omega_Q - \Omega_\Lambda}{\Omega_M}} {}_2F_1 \left(\frac{1}{2}, \frac{1}{6}, \frac{7}{6}; -\left(\frac{\Omega_\Lambda}{\Omega_M} \right) \right)$, with $\bar{Q} = \sqrt{\frac{8\rho_C}{3H_0^2}}$.

By using numerical computations, we can plot the scalar potential V_Q as a function of the scalar field Q . Figure 2 shows the plot for three different values of the parameter density Ω_Q , ($\Omega_Q = 0.75, 0.85$ and 0.95). The other parameters, Ω_M and Ω_Λ are fixed at values 0.35 and 0.65, respectively. Note that at sufficiently higher values of Q the potential approaches a constant value given by $3\bar{V}_Q \Omega_\Lambda$. This value becomes independent of the parameter Ω_Q .

3.3 The Quintessence (or Dark Energy) Cold Dark Matter Model (χ CDM)

In this case we consider the following constraint equation:

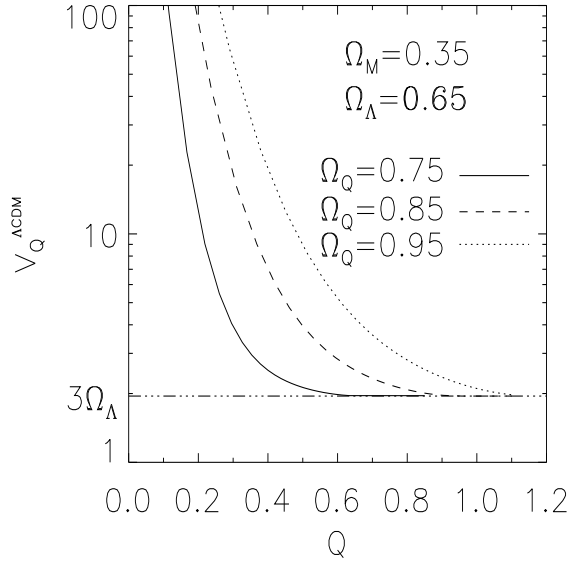


Figure 2. Plot of the scalar potential V_Q (in units of $\bar{V}_Q \equiv \rho_C/3$) as a function of the scalar field Q (in units of $\bar{Q} \equiv \sqrt{8\rho_C/3H_0^2}$) for three different values of the density parameter, Ω_Q ($\Omega_Q = 0.75, 0.85$ and 0.95). We have taken $\Omega_M = 0.35$ and $\Omega_\Lambda = 0.65$.

$$\Omega_Q \left(\frac{\rho_Q}{\rho_Q^0} \right) + \Omega_c \left(\frac{a_0}{a} \right)^2 = \Omega_\chi \left(\frac{\rho_\chi}{\rho_\chi^0} \right), \quad (21)$$

which reduces the time-time component of Einstein equations to

$$H^2 = H_0^2 \left[\Omega_M \left(\frac{a_0}{a} \right)^3 + \Omega_\chi \left(\frac{\rho_\chi}{\rho_\chi^0} \right) \right], \quad (22)$$

where, just as before, we have considered dust to be the regular matter, ρ_M .

These two latter equations together with the evolution equations for the scalar fields χ and Q form the basic set of equations for our model. In order to solve this set of equations, we need to introduce the equations of state for the quintessence scalar field components Q and χ . We assume that the χ field component is characterized by a constant equation state parameter that lies in the range $-1 < w_\chi < -0.6$. Instead, we consider w_Q to be a variable quantity whose actual value lies in the same range as w_Q .

We can use the definition of P_χ and ρ_χ in terms of the scalar field χ , together with the equation of state that relates these quantities, for obtaining χ field as a function of the scale factor a . The result is

$$\chi(a) = \chi_0 \left(\frac{a}{a_0} \right)^{-3w_\chi/2} \times \left[\frac{{}_2F_1\left(\frac{1}{2}, \frac{1}{2}, \frac{3}{2}; -\left(\frac{\Omega_\chi}{\Omega_M}\right) \left(\frac{a}{a_0}\right)^{-3w_\chi}\right)}{{}_2F_1\left(\frac{1}{2}, \frac{1}{2}, \frac{3}{2}; -\left(\frac{\Omega_\chi}{\Omega_M}\right)\right)} \right], \quad (23)$$

where χ_0 is given by $\chi_0 = \tilde{\chi} {}_2F_1\left(\frac{1}{2}, \frac{1}{2}, \frac{3}{2}; -\left(\frac{\Omega_\chi}{\Omega_M}\right)\right)$, with $\tilde{\chi} = \sqrt{4\rho_c/9H_0^2} \sqrt{\Omega_\chi(1+w_\chi)/\Omega_M w_\chi^2}$.

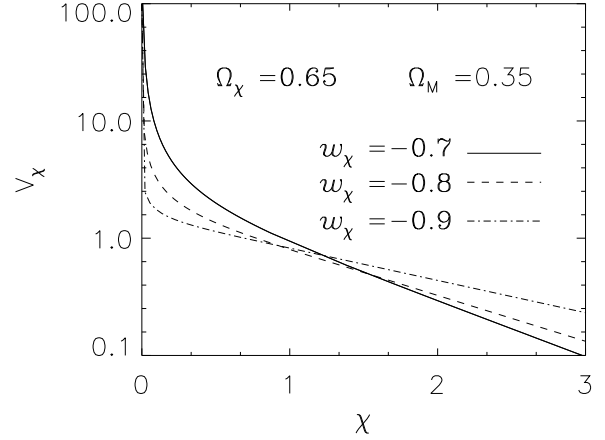


Figure 3. This graph shows the scalar potential V_χ (in units of $\rho_C/2$) as a function of the scalar field χ (in unit of $\sqrt{4\rho_C/9H_0^2}$) for three different values of the equation state parameter, $w_\chi = -0.7, -0.8$ and -0.9 . Here, we have taken $\Omega_M = 0.35$ and $\Omega_\chi = 0.65$.

In a similar way we obtain

$$V_\chi(a) = V_\chi^0 \left(\frac{a_0}{a} \right)^{3(1+w_\chi)}, \quad (24)$$

for the scalar potential V_χ as a function of the scale factor a , where the present value of this potential is given by $V_\chi^0 = \frac{1}{2}(1-w_\chi)\rho_C\Omega_\chi$.

Figure 3 shows the plot of the scalar potential V_χ as a function of the scalar field χ , for different values of the state equation parameter w_χ ; and the parameters Ω_χ and Ω_M have been fixed at 0.65 and 0.35, respectively. This form of potential has been described in the literature (Saini, Raychaudhury, Sahni & Starobinski 2000). Note that, as long as $w_\chi \rightarrow -1$, the potential $V_\chi \rightarrow const. \equiv \rho_C \Omega_\chi$, i.e., the model becomes equivalent to the Λ CDM.

Following an approach analogous to that done in the previous subsection, we find that w_Q is given by

$$w_Q^{CDM}(a) = -|w_Q^0| \left(\frac{1+\beta}{1-3\beta w_\chi} \right) \times \left[\frac{1-3\beta w_\chi \left(\frac{a}{a_0}\right)^{-3w_\chi-1}}{1+\beta \left(\frac{a}{a_0}\right)^{-3w_\chi-1}} \right], \quad (25)$$

where $\beta = \Omega_\chi/(\Omega_Q - \Omega_\chi)$ and w_Q^0 is the present value of $w_Q(a)$ defined by $w_Q^0 = P_Q^0/\rho_Q^0$. Figure 4 shows its dependence on the redshift z defined as $z \equiv a_0/a - 1$, for three different values of w_χ . As before, we have chosen $\Omega_Q = 0.85$ and $\Omega_\chi = 0.65$.

In this case the scalar field Q becomes given by

$$Q(a) = \bar{Q} \int_0^{a/a_0} \sqrt{\frac{1 + \frac{3}{2}\beta(1+w_\chi)x^{-(1+3w_\chi)}}{x + \frac{\Omega_\chi}{\Omega_M}x^{-(1+3w_\chi)}}} dx, \quad (26)$$

where $\bar{Q} = \sqrt{\frac{1}{4\pi G} \left(\frac{\Omega_Q - \Omega_\chi}{\Omega_M} \right)}$.

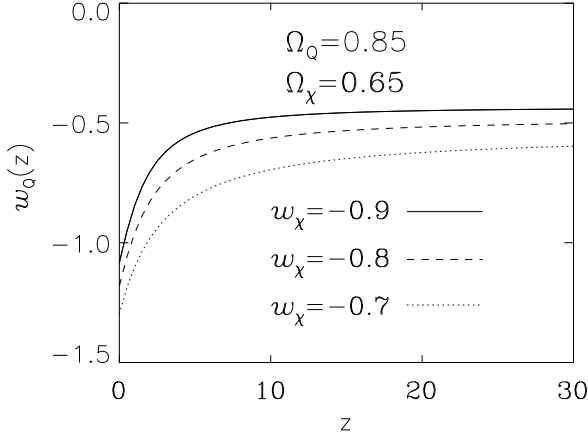


Figure 4. This plot shows w_Q (in units of $|w_Q^0|$) as a function of the redshift z for three different values of the equation state parameter, $w_\chi = -0.7, -0.8, -0.9$. We take $\Omega_Q = 0.85$ and $\Omega_\chi = 0.65$.

On the other hand, the scalar potential $V_Q^{sCDM}(a)$ is given by

$$V_Q^{sCDM}(a) = V_Q^0 \left(\frac{a_0}{a} \right)^2 \times \left[\frac{4 + 3\beta(1 - w_\chi) \left(\frac{a}{a_0} \right)^{-(1+3w_\chi)}}{4 + 3\beta(1 - w_\chi)} \right], \quad (27)$$

where $V_Q^0 = \frac{\rho_C \Omega_Q}{2(1-w_\chi)} [4/3 + \beta(1 - w_\chi)]$.

Figure 5 shows the scalar potential V_Q^{sCDM} (in units of $\rho_C/2$) as a function of the scalar field Q (in units of $1/\sqrt{4\pi G}$) for three different values of the parameter w_χ ($w_\chi = -0.7, -0.8, -0.9$). Here, we have taken $\Omega_Q = 0.85$, $\Omega_M = 0.35$ and $\Omega_\chi = 0.65$.

Note that this scalar potential decreases when Q increases. This potential asymptotically tends to vanishing for $a \rightarrow \infty$. This implies that, asymptotically, the effective equation of state becomes $P_Q = \rho_Q$ (for $\dot{Q} \neq 0$), corresponding to a stiff fluid.

4 THE FIRST DOPPLER PEAK OF THE CMB SPECTRUM

In this section, we are going to describe the position of the first Doppler peak (l_{LS}) for the different models studied in the previous section.

The scales, which are important in determining the shape of the CMB anisotropy spectrum are the sound horizon d_s at the time of recombination, and the angular diameter distance d_A to the last scattering surface. The former defines the physical scales for the Doppler peak structure that depends on the physical matter density (Ω_M), but not on the value of the cosmological constant (Ω_Λ) or spatial curvature (Ω_C), since these are dynamically negligible at the time of recombination (Efstathiou & Bond 1998). The latter depends practically on all of the parameters and is given by (for a closed universe):

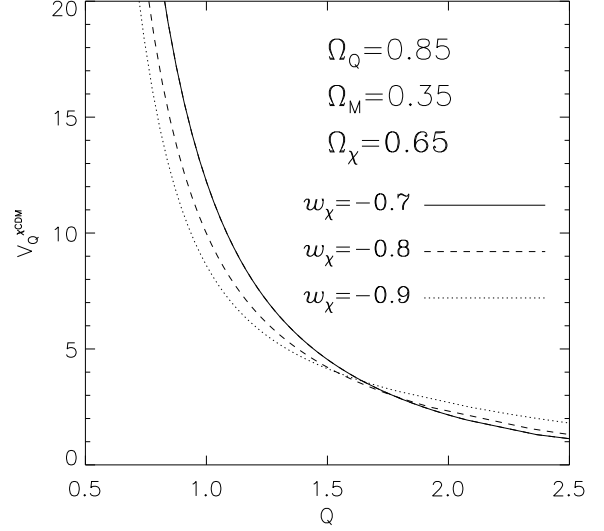


Figure 5. This plot shows V_Q (in units of $\rho_C/2$) as a function of the scalar field Q (in units of $1/\sqrt{4\pi G}$) for three different values of the equation state parameter, $w_\chi = -0.7, -0.8, -0.9$. Here, we have taken the values $\Omega_Q = 0.85$, $\Omega_\chi = 0.65$ and $\Omega_M = 0.35$.

$$d_A = \frac{1}{H_0(1+z_{LS})} \frac{1}{\sqrt{|\Omega_C|}} \sin\left(\sqrt{|\Omega_C|} y_{LS}\right), \quad (28)$$

with y_{LS} determined from

$$y_{LS} = H_0 \int_{x_{LS}}^1 \frac{dx}{x^2 H(x)}, \quad (29)$$

where $x = a/a_0$ and $H(x)$ is the Hubble parameter obtained from the time-time component of the Einstein equations. We may write for the localization of the first Doppler peak

$$l_{LS} \propto \frac{d_A}{d_S},$$

where the constant of proportionality depends on both the shape of the primordial power spectrum and the Doppler peak number (Hu & White 1996). Since we are going to keep the Ω_M parameter fixed, we shall take $l_{LS} \approx d_A$, up to a factor that depends on Ω_M and z_{LS} only.

For the $sCDM$ model we find that

$$l_{LS}^{sCDM} \approx \frac{1}{H_0(1+z_{LS})} \frac{1}{\sqrt{\Omega_M}} \times \sin \left[2 \sqrt{\frac{\Omega_Q}{\Omega_M}} \left(1 - \frac{1}{\sqrt{1+z_{LS}}} \right) \right]. \quad (30)$$

Note that, for $\Omega_Q \ll \Omega_M$ (which means that the curvature term is very small), we find that $l_{LS}^{sCDM} \sim 1/\sqrt{\Omega_M} = 1/\sqrt{\Omega_T}$ which agrees with the result obtained by Frampton *et al* (Frampton, Ng & Rohm 1998) for $\Omega_\Lambda = 0$.

In the ΛCDM model, we find that

$$l_{LS}^{\Lambda CDM} \approx \frac{1}{H_0(1+z_{LS})} \frac{1}{\sqrt{\Omega_Q - \Omega_\Lambda}} \times \sin \left[\sqrt{\Omega_Q - \Omega_\Lambda} \int_0^1 \frac{dx}{\sqrt{\Omega_M x + \Omega_\Lambda x^4}} \right], \quad (31)$$

where we have set the lower limit on the integral equal to zero, since $z_{LS} \gg 1$, and therefore we may take $x_{LS} \equiv 1/(1+z_{LS}) \approx 0$.

From the equation $\Omega_Q + \Omega_C = \Omega_\Lambda$ together with the expression $\Omega_M + \Omega_\Lambda = \Omega_T = 1$, we may write $\Omega_C = 1 - \Omega_M - \Omega_Q$. Now, following Wienberg (Weinberg 2000), we will keep fixed the Ω_M parameter with Ω_T close to one and Ω_Q close to Ω_Λ . Thus, we find that

$$l_{LS}^{\Lambda CDM} \sim \Omega_T^{-\eta}, \quad (32)$$

where

$$\eta = \left(\frac{\partial \ln l_{LS}^{\Lambda CDM}}{\partial |\Omega_C|} \right)_{\Omega_\Lambda=1-\Omega_M} = \frac{1}{6} \mathcal{I}_1^2 - \frac{1}{2} \frac{\mathcal{I}_2}{\mathcal{I}_1}, \quad (33)$$

with

$$\mathcal{I}_1 \equiv \int_0^1 \frac{dx}{[(1-\Omega_M)x^4 + \Omega_M x]^2}, \quad (34)$$

and

$$\mathcal{I}_2 \equiv \int_0^1 \frac{x^4 dx}{[(1-\Omega_M)x^4 + \Omega_M x]^3}. \quad (35)$$

These expressions yield $\eta = 2.45$ for $\Omega_M = 0.2$ and $\eta = 11/18$ for $\Omega_M = 1.0$. The latter value should be compared with that corresponding to the $\Omega_\Lambda = 0$ case, in which $\eta = 1/2$.

For the χCDM model we find that

$$l_{LS}^{\chi CDM} \approx \frac{1}{H_0(1+z_{LS})} \frac{1}{\sqrt{\Omega_Q - \Omega_\chi}} \times \sin \left[\sqrt{\Omega_Q - \Omega_\chi} \int_0^1 \frac{dx}{\sqrt{\Omega_M x + \Omega_\chi x^{1-3w_\chi}}} \right], \quad (36)$$

Following an approach similar to that described above, we now use $\Omega_Q + \Omega_C = \Omega_\chi$ together with $\Omega_M + \Omega_\chi \equiv \Omega_T = 1$ and, taking Ω_Q close to Ω_χ , we find an expression similar to eq. (32), with η given by eq. (33), but now the integrals are given by

$$\tilde{\mathcal{I}}_1 \equiv \int_0^1 \frac{dx}{[(1-\Omega_M)x^{1-3w_\chi} + \Omega_M x]^2}, \quad (37)$$

and

$$\tilde{\mathcal{I}}_2 \equiv \int_0^1 \frac{x^{1-3w_\chi} dx}{[(1-\Omega_M)x^{1-3w_\chi} + \Omega_M x]^3}. \quad (38)$$

The values of the exponent η appearing in equation (32) are tabulated in table 1 for the different models treated here.

One important parameter that describes the dependence of the first Doppler peak position on the different parameters that characterize any model is the shift parameter R . This parameter is related to the geometry of the universe and, for closed models, it may be defined as (Efstathiou & Bond 1998; Melchiorri & Griffiths 2000; Melchiorri 2002)

$$R = \sqrt{\frac{\Omega_M}{|\Omega_C|}} \sin \left[\sqrt{|\Omega_C|} y_{LS} \right], \quad (39)$$

where y_{LS} is defined by equation (29).

For the sCDM model, this parameter is given by

$$R_{sCDM} = \sqrt{\frac{\Omega_M}{\Omega_Q}} \sin \left[2\sqrt{\frac{\Omega_Q}{\Omega_M}} \left(1 - \frac{1}{1+z_{LS}} \right) \right],$$

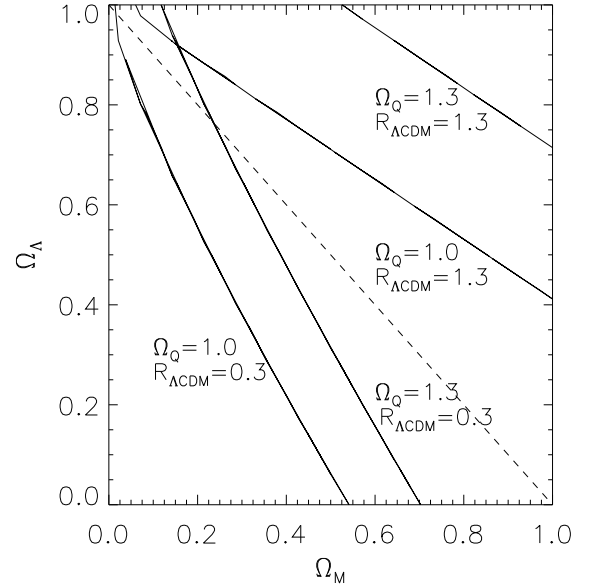


Figure 6. This plot shows a set of lines $R = \text{const.}$ for different values of the parameter Ω_Q . The values of R and Ω_Q are given next to each line. We have also included in this plot the line that joins the points $(1.0; 0.0)$ and $(0.0; 1.0)$ (dashed line).

which, at first glance, seems to be a quantity that depends on Ω_Q and Ω_M parameters. But we know that, in this model, the parameter Ω_M gets the value one. Here, we have used the equality $|\Omega_C| = \Omega_Q$.

For the ΛCDM model we find that the parameter R is given by

$$R_{\Lambda CDM} = \sqrt{\frac{\Omega_M}{\Omega_Q - \Omega_\Lambda}} \sin \left[\sqrt{\Omega_Q - \Omega_\Lambda} \times \int_0^1 \frac{dx}{\sqrt{\Omega_M x + \Omega_\Lambda x^4}} \right]. \quad (40)$$

Here, we have used the relation $|\Omega_C| = \Omega_Q - \Omega_\Lambda$ (with $\Omega_Q > \Omega_\Lambda$) and we have considered $x_{LS} \approx 0$.

In Figure 6 we have plotted a set of lines $R = \text{const.}$ for different values of the parameter Ω_Q . The values of R and Ω_Q are given next to each line. Notice that, when we increase the value of Ω_Q (by keeping the value of R fixed), the $R = \text{const.}$ lines are moved towards greater values of the Ω_M parameter. This means that the Doppler peaks are shifted towards greater angular scale values (Melchiorri & Griffiths 2000).

For the χCDM model we find that the R parameter becomes given by the following expression:

$$R_{\chi CDM} = \sqrt{\frac{\Omega_M}{\Omega_Q - \Omega_\chi}} \sin \left[\sqrt{\Omega_Q - \Omega_\chi} \times \int_0^1 \frac{dx}{\sqrt{\Omega_M x + \Omega_\chi x^{1-3w_\chi}}} \right]. \quad (41)$$

In Figure 7 we have plotted two sets of $R_{\chi CDM} = \text{const.}$ contours for three different values of w_χ ($w_\chi = -0.3, -0.5, -0.9$). In these curves we have kept fixed Ω_Q

Table 1. This table shows the exponent parameters η of Eq. (32) for the Λ CDM and the χ CDM models, where we have used different values of the parameter Ω_M . For the latter model we have taken the values -0.7, -0.8 and -0.9 for the parameter w_χ .

Ω_M	$\eta^{\Lambda CDM}$	$\eta^{\chi CDM}$		
		$w_\chi = -0.7$	$w_\chi = -0.8$	$w_\chi = -0.9$
0.2	2.422	2.152	2.258	2.346
0.3	1.727	1.571	1.633	1.684
0.4	1.350	1.248	1.289	1.322
1.0	0.595	0.571	0.581	0.588

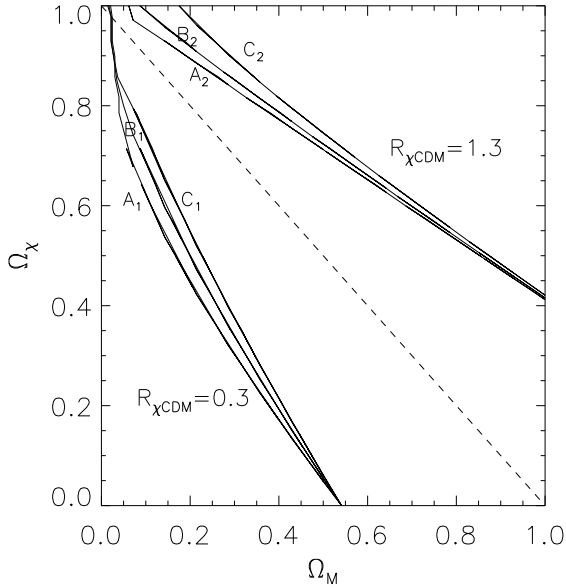


Figure 7. This plot shows two sets of lines of constant R in the $\Omega_\chi - \Omega_M$ plane for three different values of the state equation parameter; $w_\chi = -0.3$ (A_1 and A_2 lines), $w_\chi = -0.5$ (B_1 and B_2 lines) and $w_\chi = -0.9$ (C_1 and C_2 lines). The value of R is given next to each set of lines.

equal to one. Notice that, for small values of the Ω_χ , these curves almost overlaps.

We should note that the s CDM and Λ CDM models are special cases of the χ CDM model. They are obtained from equation (41) by taking $\Omega_\chi = 0$ and $\Omega_\chi = \Omega_\Lambda$ with $w_\chi = -1$, respectively. At this point, we should add that more precise future astronomical measurements of the location of the first Doppler peak (and its corresponding characteristics) will certainly supply information on which of these models (or another one) is more appropriate for describing the universe we live in.

5 CONCLUSIONS

In this paper we have described closed universe models in which, apart from the usual Cold Dark Matter component, we have included a quintessence scalar field Q . We have fine tuned the quintessence component together with the curvature term for getting a flat model in which three dif-

ferent models were described. These models were the standard Cold Dark Matter (s CDM model, characterized by $\Omega_T \equiv 1$), the Cosmological constant Cold Dark Matter (Λ CDM model, characterized by $\Omega_T = \Omega_M + \Omega_\Lambda \equiv 1$) and the Quintessence (or Dark Energy) Cold Dark Matter (χ CDM, model characterized by $\Omega_T = \Omega_M + \Omega_\chi \equiv 1$). In all of them we have described the properties of the scalar field Q . The characterization of the scalar field Q in the different models comes from the determination of the scalar potential $V(Q)$. In all of these models, this potential decreases when the scalar field Q increases. This property seems to be common to all of the dark energy potentials. In the Λ CDM model, this potential approaches a constant given by $3\sqrt{V_Q}\Omega_\Lambda$ at a large scale factor. In the other two models, the potential $V(Q)$ goes to zero, asymptotically. Since all of these models are indistinguishable from flat models at enough low redshift (say $z \sim 1$), we expect that with an appropriate fine tuning, it will be possible to consolidate the supernova measurements with closed universe models.

As an applicability of the different models described above, we have determined the position of the first Doppler peak together with the shift parameter R . For $|\Omega_C| \approx 0$, we have found that the first Doppler peak is quite sensitive to the mass density values (Ω_M).

For a fixed Ω_M at 0.4 and $\Omega_T \approx 1$, the first Doppler peak behaves as $\Omega_T^{-\eta}$, with the exponent η given by 0.500 (for the s CDM model), 1.350 (for the Λ CDM model), 1.248 (for the χ CDM model with $w_\chi = -0.7$), 1.289 (for the χ CDM model with $w_\chi = -0.8$) and 1.322 (for the χ CDM model with $w_\chi = -0.9$). We may compare these values with that specified by Weinberg, which results to be 1.244. This value agrees with that obtained from the χ CDM model, in which $w_\chi = -0.7$. Some values of the η exponent have been tabulated in table 1. In this table we have excluded the value corresponding to the s CDM model, where $\eta = 1/2$ is found. Precise measurements of the location of the first Doppler peak (together with the other peaks and their properties) can supply information on the parameters Ω_Λ (or Ω_χ) and Ω_T , from which we could obtain an appropriate value for the parameter Ω_Q .

Secondly, we have determined the shift parameter R . In the Λ CDM model, this parameter is highly sensitive to the value of Ω_Q . Something similar occurs in the χ CDM model. We have plotted curves $R = \text{const.}$ in the graph Ω_χ v/s Ω_M for different values for the w_χ parameter. For $\Omega_\chi \approx 1$ the $R = \text{const.}$ curves became separated. But, for $\Omega_\chi \approx 0$, they began to come together. It is interesting to consider the value $R = 1$, since this case allows us to determine a precise value

for the Ω_Q parameter. For the sCDM model we obtain that $\Omega_Q = 0$; meanwhile, for the other two cases, $\Omega_Q = \Omega_\Lambda$ and $\Omega_Q = \Omega_\chi$ for the Λ CDM and χ CDM models, respectively. We may conclude that, as far as we are concerned with the observed acceleration detected in the universe and the location of the first Doppler peak, we will be able to utilize a closed model to describe the universe we live in.

ACKNOWLEDGMENTS

I am grateful to Francisco Vera for plotting assistance and Paul Minning for carefully reading the manuscript. Discussion with M. Cataldo, N. Cruz, S. Lepe, F. Peña and P. Salgado are acknowledged. I also acknowledge the Universidad de Concepción and Universidad del Bio-Bio for partial support of the Dichato Cosmological Meeting, where part of this work was done. This work was supported from COMISION NACIONAL DE CIENCIAS Y TECNOLOGIA through FONDECYT Projects N^o 1000305 and 1010485 grants, and from UCV-DGIP N^o 123.752.

REFERENCES

- Caldwell R., Dave R. and Steinhardt P., 1998, Phys. Rev. Lett. 80, 82.
- Crooks J. L., Dunn J. O., Frampton P. H. and Ng Y. J., astro-ph/0005406.
- Cruz N., del Campo S. and Herrera R., 1998, Phys. Rev. D 58, 123504.
- Cataldo M. and del Campo S., 2000, Phys. Rev. D 62, 025455.
- del Campo S. and Cruz N., 2000, MNRAS, 317, 825.
- De Bernardis P. et al., 2000, Nature, 404, 955.
- Dodelson S. and Knox L., 2000, Phys. Rev. Lett., 84,3523.
- Efstathiou G. and Bond J. R., astro-ph/9807103.
- Frampton P., Ng Y. J. and Rohm R., 1998, Mod. Phys. Lett. A13, 2541.
- Garnavich P. M. *et al*, 1998, ApJ, 509, 74.
- Guth A., 1981, Phys. Rev. D, 23, 347.
- Hu W. and Sugiyama N., 1995a, ApJ, 444, 489.
- Hu W. and Sugiyama N., 1995b, Phy. Rev. D, **51**, 2599.
- Hu W., Sugiyama N. and Silk J., 1997, Nature, 386, 37.
- Hu W. and White M., 1996, ApJ, 471, 30.
- Kamionkowsky M., Spergel D. N. and Sugiyama N., 1994, ApJ, 426,L57.
- Kamionkowski M. and Toumbas N., 1996, Phys. Rev. Lett., 77, 587.
- Kochanck C. S., 1996, ApJ, 466, 638.
- Kolb E. W., 1989, ApJ, 344, 543.
- Mather J. et al., 1994, ApJ, 420, L439.
- Melchiorri A. and Griffiths L. M., astro-ph/0011147.
- Melchiorri A., astro-ph/0201237.
- Mellier Y., 1999, ARA&A, 37, 127.
- Perlmutter S. et al., 1998, Nature 391, 51.
- Roos M. and Harun-or-Rashid S., astro-ph/0005541.
- Saini T. D., Raychaudhury S., Sahni V. and Starobinski A.,2000, Phys. Rev. Lett., 85, 1162.
- Wang L., Caldwell R. R., Ostriker J. P. and Steinhardt P. J., 2000, ApJ, 530, 17.
- Weinberg S., 2000, Phys. Rev. D, 62, 127302.
- White S. et al., 1993, Nature, 366, 429.